Journal of Computer Science and Cybernetics, V.33, N.4 (2017), 289–307
DOI 10.15625/1813-9663/33/4/10835

DESIGNING OPTIMAL FUZZY CONTROLLER FOR MRD-BASED TRAIN-CAR SUSPENSION SYSTEMS

SY DZUNG NGUYEN[1], BAO DANH LAM[2]

[1]*Division of Computational Mechatronics, Institute for Computational Science, Ton Duc Thang University, Ho Chi Minh City, Viet Nam*
[2]*Faculty of Electrical and Electronics Engineering, Ton Duc Thang University, Ho Chi Minh City, Viet Nam*
[1]*nguyensydung@tdt.edu.vn*

Abstract. Random time-varying chassis mass, which consists of passenger and cargo mass as well as the normalized wind force, causes reducing the effectiveness of smart vehicle suspensions. In order to deal with this, we develop a novel fuzzy-based dynamic inversion controller (FDIC) for the control of a train-car suspension system using a magneto-rheological damper (MRD) or MRDs. The FDIC is constituted of three main parts: i) an inverse MRD model (ANFIS-I-MRD) via a measured data set and an adaptive neuro-fuzzy inference system (ANFIS), ii) a fuzzy-based sliding mode controller (FSMC) and iii) a disturbance and uncertainty observer (DUO). The FSMC is designed via the two following steps. The first one is to establish and optimize parameters of a sliding mode controller (SMC). The next is to design a fuzzy logic system to expand the ability of the SMC to face with the larger ranges of the load variation. The DUO is used to compensate for disturbance and uncertainty. By using the ANFIS-I-MRD and the control force estimated by the FDIC, current for the MRD at each time for stamping out chassis vibration is specified. The stability of the FDIC is analyzed via Lyapunov stability theory. Surveys have shown that the FDIC could provide the improved control competence to reduce unwanted vibrations in an enlarged range of the varying chassis load.

Keywords. Fuzzy sliding mode control; Fuzzy control; Sliding mode control; Compensating for Disturbance and uncertainty.

1. INTRODUCTION

Vehicle suspensions using MRDs have been widely applied as an effective device to improve both ride quality and safety of passenger cars and high-speed railroad vehicles. In these systems, damping force generated by the MRDs can be controlled by the intensity of magnetic field [1, 2, 3, 4, 5, 6, 7]. It has been known that in order to enhance performance in the real field, several issues should be carefully considered, including the solutions for fast response, easy controllability, robustness against uncertainty and disturbance (UAD) and accurate identification of the hysteretic dynamic behavior of MRDs [1, 8]. A becoming control strategy needs to be developed to provide an appropriate time-varying control force to minimize the vibration of the chassis. Generally, all real suspension systems are always subjected to UAD. As an essential tool for improving the system effectiveness, compensating for UAD needs to be also paid attention to. UAD may come from inexactly established

models of the control plants, the lack of accuracy of the measurement devices, and unknown nonlinear characteristics of the actuators. It may also derive from the time varying characteristics of the control plants. In [7], the sprung mass was considered as an aspect taking part in UAD. The chassis mass varies frequently due to many reasons such as the change of passengers, load mass and wind load. Besides, the unknown influence of environmental conditions on the system can also affect negatively on control systems. To face with these, sliding mode control technique (SMCT), fuzzy logic (FL), and artificial neural networks (ANN) together with solutions for noise compensation have been widely developed [9, 10, 11, 12, 13, 14, 15, 16, 17, 18, 19, 20, 21, 22, 23, 24, 25, 26].

It is well-known that the SMCT owns several benefits such as the ability to adapt itself to the impact of noise, the insensitivity to the external effects as well as the simplicity of implementation. The first step to formulate SMC is to build a sliding surface in the state space domain. For this, the approaching and maintaining phases are performed during the operating process to establish and maintain a reasonable operating status. In the first phase, system's dynamic response expressed via a state space is controlled to direct towards the sliding surface. Then, in the second phase, when this process reaches the surface, the system dynamic response is upholden along the surface to keep all of system's states on the switching surface [9]. This guarantees the stability of the control system. However, there is an issue related to the fact that this process, as usual, needs an infinite commutation function working as an adaptive compensator with a high frequency of the change in the control signal. As a result, the chattering phenomenon may appear and damage the system [27]. To prevent the chattering problem, many approaches have been proposed such as building adaptive structures [7, 16, 28], the integrating FL and/or ANN into sliding mode control system (SMCs) [9, 25, 27, 29, 30].

The ability to reach the sliding surface and keep the system states on it without chattering reflects the SMCs quality. Reality shows that an appropriate combination of SMCs and the other models may create novel capabilities for SMCs to get the target. The well-known combination of SMCs and FL in the model named FSMC brings the control system the essential strong points together with the arisen disadvantages. In this model, the FL can provide useful solutions for function approximation with a high degree of flexibility along with a vigorous tool for information inference [8, 12]; while the sliding mode approach can create adaptive control laws based on its thorough stability analysis capability [7, 9, 10, 18]. In this tendency, optimization methods such as the Evolutionary Algorithm (EA), Differential Evolution (DE) [31, 33] or the algorithm rank-DE [34] could be employed to improve the system performance. Such advantages of the FSMC model have been effectively exploited in many fields, including suspension systems [15, 16, 20]. FSMC owns the advantages, this, however, may increase the time delay due to the high calculating cost in some cases [23].

In [15], an adaptive SMCs based on the Takagi–Sugeno (T–S) fuzzy approach was presented. The varying of sprung and unsprung masses in the given ranges was viewed as uncertainty aspects. The T–S fuzzy system described the system in the presence of UAD. Relied on this fuzzy model, the adaptive FSMC was built to set up the control law. Although the method can exploit the advantages of both SMCs and FL, the T-S model with various parameters needing to be estimated online takes part in expanding time delay. In real-time control systems, this is one of the main causes of reducing the control quality [9, 23]. Another FSMC-based control strategy can be referred in [16]. An adaptive FSMC for vehicle

suspension systems subjected to the system time-varying and nonlinear uncertainty behaviors was shown. It combined an adaptive fuzzy rule structure (AFRS) with SMCs. In the AFRS, the sliding surface was employed as a one-dimensional fuzzy input variable. Being viewed as a becoming solution for improving calculating cost, this however could not fully exploit the varying tendency of the sling surface to adjust appropriately the control law. In [20], a FSMC for an active suspension system was presented. In this, the sliding surface and its change were employed as input variables of a traditional fuzzy controller to update the control law. This can partly overcome the issue related to the one-dimensional fuzzy input variable of [16] as mentioned above, however the effectiveness of the method become worse quickly if the UAD amplitude varied fast. More recently, in [7] the authors introduced a SMCT-based controller for active suspension system of train vehicles subjected to UAD. In this work, adaptive adjusting the slope of the sliding surface was performed to provide a smooth control signal without the chattering phenomenon. Designed via the ideal operating condition corresponding to the normal load, the method, hence, does not match well with the change of the load amplitude. Consequently, the technical originality of this work is to propose a new controller for MRD-based train-car suspensions subjected to random time-varying chassis mass in enlarged ranges, which is a fuzzy-based dynamic inversion controller named FDIC. It is constituted of an inverse MRD model using an ANFIS (ANFIS-I-MRD), a fuzzy-based optimal sliding mode controller, FSMC, and a nonlinear disturbance and uncertainty observer, NUO. First, in the presence of the normal load, by using Lyapunov stability theory and the algorithm rank-DE [34], an optimal structure of the sliding mode controller (SMC) is built. An optimal FL system (FLS_{op}) is then designed to expand the ability of the SMC to deal with the larger varying ranges of the chassis mass. The NUO presented in [1] is then used to calculate the compensating force for UAD. The ANFIS-I-MRD, which is based on a measured data set expressing dynamic response of the MRD, is employed to specify current supporting the MRD to generate the required control force estimated by the FSMC and NUO, in total. Finally, surveys for evaluating the method are carried out together with the comparison with the results from another controllable system and the passive one.

The two main contributions of this work are as follows. The first one is to propose the FSMC for improving the competence to adapt to the random chassis mass. The FSMC relies on the framework created by the optimal SMC and the adaptive fuzzy inference laws of the FLS_{op} in order to expand UAD's permitted varying range. Seen as the second contribution is the ANFIS-I-MRD built via a real MRD and an experimental apparatus.

2. CONTROL STRATEGY

Fig. 1 shows the quarter model of a semi-active MRD train-car suspension system. It is noted here that in trains two suspension systems are normally used; one is installed for vertical chassis vibration control as shown in Fig. 1 while the other is to stamp out its transversal vibration. In this work, the first system is considered. The chassis mass $m_s(t)$ is varied due to many reasons such as the change in the passengers and load mass as well as the normalized impact of wind on the train. The unsprung mas m_u consisting of the mass of the wheel, shaft, brake and suspension linkage is assumed to be a constant parameter. In this model, u is the control force generated by the semi-active actuator, MRD; k_s is the stiffness coefficient of the linear spring; k_t is the wheel deflection stiffness; c_s is the damping

coefficient of the suspension; c_t is the damping coefficient of the wheel. Displacement of $m_s(t)$ and m_u are presented by z_s and z_u, respectively, while the vertical track-profile disturbance denoted by z_y. Parameters $f_s,\ f_{ts},\ f_d,\ f_{td}$ respectively denote sprung and damper forces corresponding to $k_s,\ k_t, c_s,\ c_t$.

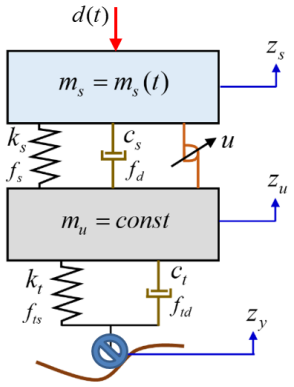

Figure 1. Quarter train-car MRD suspension model

A state vector x(t) is expressed as below

$$x(t) = [x_1 \quad x_2 \quad x_3 \quad x_4]^T, \tag{1}$$

$$x_1 = x_s; \quad x_2 = \dot{x}_s; \quad x_3 = z_u; \quad x_4 = \dot{z}_u. \tag{2}$$

Let m_m be the maximum chassis mass defining the maximum passenger and load mass; $\delta m(t)$ be the normalized wind load; $\Delta m(t)$ be the less passenger and load mass than m_m. By applying $x(t)$ as in (1) and Newton's second law, we get the dynamic equation of the system in the presence of UAD as follows:

$$m_m(t)\ddot{z}_s + f_s(x,t) + f_d(x,t) = -u(t) + d(t), \tag{3}$$

where,

$$f_s = k_s(x_1 - x_3); \quad f_d = c_s(x_2 - x_4); \quad f_r = f_{ts} + f_{td} = k_1(x_3 - z_y) + c_t(x_4 - \dot{z}_y). \tag{4}$$

In (3), the uncertainty aspect depicted in $d(t)$ relates mainly to the difference $\Delta m(t)$ between m_m and the real chassis mass (or the real sprung mass) $m_s(t)$ actually impacting on the system at time t. While the disturbance aspect participating in $d(t)$ mainly derives from the unknown impact of the normalized wind load $\delta m(t)$ as well as from the vertical disturbance exciting of the track profile which cannot be accurately measured during the operating process. Now, using expressions from (1) to (4), the state space model can be written as follows

$$\begin{cases} \dot{x}(t) = f(x,t) + g_1(x,t)u(t) + g_2 d(t) \\ y(t) = x_1(t), \end{cases} \tag{5}$$

where

$$f(x,t) = \begin{bmatrix} x_2(t) \\ \frac{1}{m_m}(-f_s - f_d) \\ x_4(t) \\ \frac{1}{m_u}(f_s + f_d - f_{ts} - f_{td}) \end{bmatrix}; \quad g_1 = \begin{bmatrix} 0 \\ -\frac{1}{m_m} \\ 0 \\ +\frac{1}{m_u} \end{bmatrix}; \quad g_2 = \begin{bmatrix} 0 \\ \frac{1}{m_m} \\ 0 \\ +\frac{1}{m_u} \end{bmatrix}. \tag{6}$$

The semi-active control force $u = u(t)$ in (5) needs to be estimated such that vertical acceleration of the chassis is extinguished as much as possible. With this purpose, we propose a control strategy relied on SMCT, ANFIS, and the lumped UAD quantity as in Fig. 2. The method is described upon two phases. The first one is to design a nonlinear controller for the system without UAD, to which we obtain the controller FSMC for calculating the principal control force part $u_s(t)$. The second phase is to establish NUO to observe $u_c(t)$ for compensating for UAD. As a result, semi-active control force $u(t) = u_s(t) + u_c(t)$ is estimated. Finally, based on the ANFIS-I-MRD, current supporting the MRD to generate the $u(t)$ is specified, $I(t)$ =ANFIS$(u(t))$ $\equiv$ ANFIS-I-MRD$(u(t))$.

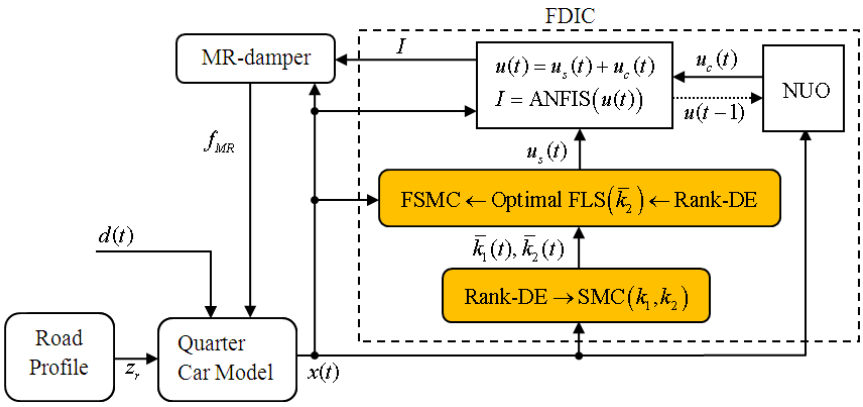

Figure 2. Structure and operating principle of the FDIC

3. DESIGNING THE FDIC

3.1. Building the ANFIS-I-MRD

The ANFIS-I-MRD is built via two steps. The first one is to build a data set expressing dynamic response of the MRD, while the second one is to identify the MRD upon the data and an ANFIS. For the data set, $\begin{bmatrix} x_{i1} & x_{i2} & x_{i3} \end{bmatrix} \equiv \begin{bmatrix} d_{re_i} & v_{re_i} & f_{MR_i} \end{bmatrix}$is defined as the input, while $y_i = I_i$ is the output of the i^{th} sample. Where, $d_{re_i} = (x_1 - x_3)$ is the relative displacement and velocity between chassis and unsprung mass; I_i is the current applying to the MRD to generate the damping force f_{MR_i} corresponding to d_i, v_i at the i^{th} instant. Based on the obtained data set and the recurrent mechanism and impulse noise filter for establishing ANFIS presented by Nguyen et al. in [35], the ANFIS-I-MRD is established.

Fig. 3 shows an experimental apparatus for building the data set. The load cell is fixed to the piston shaft of the MRD and directed by the upper bed to connect to the shaft of the DC servo motor via the translating rod. The cylinder of the MRD is fixed to the lower bed. Based on the eccentric mass, the rotation of the motor shaft is transformed into the translation motion of the damper piston. The signal from the load cell, damping force f_{MR} generated by the MRD, is then sent to the computer via the A/D converter and signal processing equipment. By adjusting the rotation velocity ω of the DC motor using the computer and motor driver, and also by adjusting the current I supporting the MRD, we obtain the corresponding damping force f_{MR} at each sampling time.

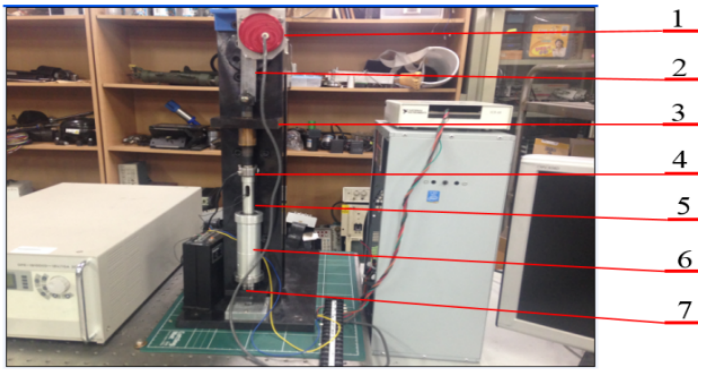

Figure 3. Experimental apparatus for building the data set: 1-eccentric mass, 2-translating rod, 3-upper bed, 4-load cell, 5-piston shaft, 6-MRD, 7-lower bed

3.2. Designing the FSMC

The FSMC is constituted of two parts: the optimal sliding mode controller (SMC) and the optimal FLS$_{op}$. First, in the presence of the normal load, by using Lyapunov stability theory and the rank-DE [34], the optimal structure of the SMC is built. The FLS$_{op}$ is then designed to expand the ability of the SMC to deal with the larger varying amplitudes of the chassis mass.

Firstly, the initial SMC is built as in [1] via a sliding surface as follows

$$S(t) = k_1 x_1(t) + x_2(t), \tag{7}$$

where, k_1 is the positive coefficient. From (7), the following is obtained

$$\dot{S}(t) = \frac{dS}{dt} = k_1 \dot{x}_1(t) + \dot{x}_2(t) = k_1 x_2(t) + \dot{x}_2(t). \tag{8}$$

From (8), (2)-(6) we have

$$\dot{S}(t) = k_1 x_2 + \frac{1}{m_m}[-f_s - f_d - u(t) + d(t)]. \tag{9}$$

A Lyapunov candidate function $V(x) = 0.5\, S(t)^2$, to which $\dot{V}(x) = S(t)\dot{S}(t)$, is employed. It can infer that in order to meet the Lyapunov stability condition, the control law must be

established such that the following clause is satisfied

$$\dot{S}(t) = -k_2(t)\,\mathrm{sat}(S(t)), \tag{10}$$

where $k_2(t)$ is the positive coefficient used to adaptively adjust the slope of $S(t)$.

Due to $\dot{V}(x) = S(t)\dot{S}(t)$, from (10) we can infer the following relation

$$\dot{V}(S(t)) = -k_2\,|S(t)| \leq 0,\ \forall k_2(t) \geq 0. \tag{11}$$

Be noted $V(x) \geq 0\ \forall x$ and $V(0) = 0$, based on (11) it can conclude that the dynamics of the $S(t) \to 0$ is an asymptotically stable Lyapunov process. This means the control force for the suspension such that the chassis vibration converges to zero stably can be inferred from (9) and (10) as below

$$u(t) = m_m k_1 x_2(t) - f_s - f_d + m_m k_2\,\mathrm{sat}(S(t)) + d(t). \tag{12}$$

Using the estimated value $\hat{d}(x,t)$ of $d(x,t)$ quantified by the NUO, the control force can be depicted as

$$u(t) = m_m k_1 x_2(t) - f_s - f_d + m_m k_2\,\mathrm{sat}(S(t)) + \hat{d}(t). \tag{13}$$

Be noted, the control quality of the SMC depicted in (13) deeply depends on $\hat{d}(t)$, k_1 and k_2. Changing too frequently of $u(t)$ due to k_2 and function sat() may result in the chattering phenomenon. In the rest of this section, improving the SMC upon k_1 and k_2 to adapt to UAD is presented. By which the optimal parameter of k_1 signed $\bar{k}_1$ and the adaptive parameter of k_2 signed $\bar{k}_{2ad}(t)$ are obtained.

Expressions (10) shows that $k_2(t)$ is proportional to not only value of $\left|\dot{S}(t)\right|$ but also the quantity of $S(t)$. Therefore, we propose an optimal fuzzy logic system signed FLS_{op} for setting up $\bar{k}_{2ad}(t)$ as follows

$$k_2 \equiv \bar{k}_{2ad}(t) = FLS_{op}\left(S(t), \dot{S}(t)\right). \tag{14}$$

The FLS_{op} is designed by two steps as below.

Step 1. Optimizing structure of the SMC in the ideal operating condition:

From (13), by using the ideal operating condition depicted by the maximum chassis mass m_m without UAD, the suspension system is controlled via the following law

$$u(t) = m_m k_1 x_2(t) - f_s - f_d + m_s k_2\,\mathrm{sat}(S(t)). \tag{15}$$

Based on (15), k_1 and k_2 are then optimized using algorithm rank-DE [34] with an objective function $J(k_1, k_2)$ defined as follows

$$J(k_1, k_2) = \max(|\dot{x}_2(t)|) \to \min. \tag{16}$$

Thus, optimal parameters $\bar{k}_1$ and $\bar{k}_2$ of k_1 and k_2 respectively are addressed.

It should be noted that $\bar{k}_1$ and $\bar{k}_2$ as above mentioned only match with the ideal condition. This operating condition is however different from the real one, to which the $m_s = m_s(t)$ as well as UAD always exist. To overcome this, the next step is then performed.

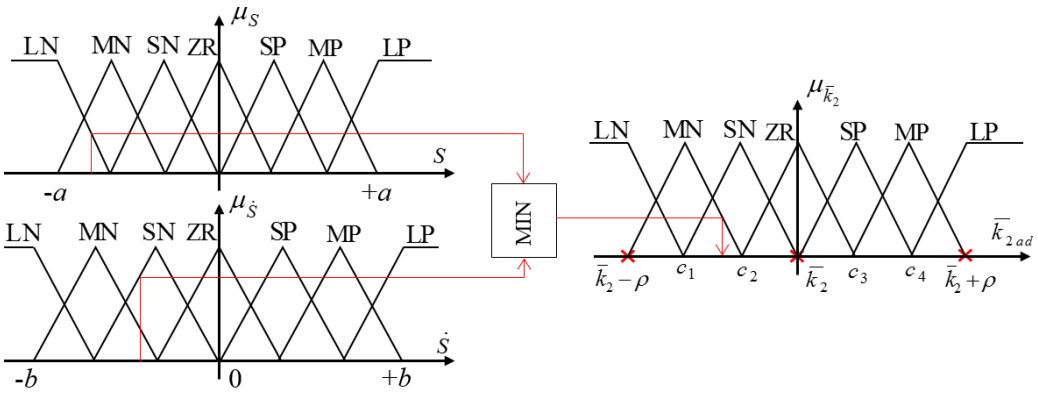

Figure 4. The input fuzzy sets and the initial structure of the output fuzzy sets of the FLS: a and b are specified based on simulation via the violent operating conditions of the system while the optimal values of $c_i, i = 1...4$, are specified via the algorithm rank-DE

Step 2. Designing the FLS_{op} in an adaptable range centered by $\bar{k}_2$ to specify $\bar{k}_{2ad}(t)$. This work is carried out as follows:

1) *Building fuzzy set structures*

The fuzzy set structures of the FLS are illustrated in Fig. 4.

In the output space, $\bar{k}_2$ is used as a distribution center, by which $k_2(t) \equiv \bar{k}_{2ad}(t)$ is an adaptive value belonging to $[\bar{k}_2 - \rho, \bar{k}_2 + \rho]$, where $0 < \rho < \bar{k}_2$ is an adaptive coefficient chosen by the designer. For example, for the surveys in Section 4 we chose $\rho = 0.95\,\bar{k}_2$ with seven output fuzzy sets named large-negative (LN), medium-negative (MN), small-negative (SN), zero (ZR), large-positive (LP), medium-positive (MP), small-positive (SP). In the input space, the input fuzzy sets are named to be the same. The parameters a and b are specified by loops with two following steps for each loop. In the first step of the first loop, they are default options to perform the second step: specifying them via simulation surveys. While, in the first step of the next loops, they are the results of the previous loop. We obtain these parameters when the process converges. For example, as presented in Section 4, tracks No. 1 and 3 were employed in this work, by which we had $a = 4.2$; $b = 5.4$.

2) *Optimizing the output fuzzy set structure to set up the* FLS_{op}

The optimal values of c_i, $i = 1...4$ are then estimated via the algorithm rank-DE [34] with the objective function defined as follows

$$J(c_i,\, i = 1...4) = \max(|\dot{x}_2(t)|) \to 0. \tag{17}$$

3) *Determining the control law*

Based on Lyapunov stability analysis as mentioned in Subsection 3.2, it is inferred that the fuzzy inference laws have to make the system states reach to the condition $S(t)\,\Delta S(t) < 0$. There are relations as follows, $\dot{S}(t)$ or $\Delta S(t)$ increases as $u(t)$ increases. In case $S(t) > 0$, if $u(t)$ increases then $S(t)\,\Delta S(t)$ reduces while in case $S(t) < 0$, if $u(t)$ reduces then $S(t)\,\Delta S(t)$ reduces [36]. These are expressed via fuzzy rules given in Table 1.

Remark 1. The above analysis reflects that $\Delta S(t)$ or $\dot{S}(t)$ should be used to establish fuzzy inference laws so as to exploit fully their varying tendencies to improve the effectiveness of

Table 1. Fuzzy rules of the FL

$\dot{S}(t)$ \ $\bar{k}_{2ad}(t)$, S	**LN**	**MN**	**SN**	**ZR**	**SP**	**MP**	**LP**
LN	LN	LN	MN	SN	NC	NC	NC
MN	LN	MN	SN	ZR	NC	NC	NC
SN	MN	SN	SN	ZR	NC	NC	NC
ZR	SN	SN	SN	ZR	SP	SP	SP
SP	NC	NC	NC	ZR	MN	SP	MP
MP	NC	NC	NC	ZR	SP	MP	LP
LP	NC	NC	NC	SP	MP	LP	LP

the updating control law. In view of this, the solution based on the one-dimensional fuzzy input variable for reducing the time delay as presented [16], to which $S(t)$ is employed only to update $u(t)$, is hence not an optimal option. Instead of this way, based on both $S(t)$ and $\dot{S}(t)$ we set up states NC (No Change) as given in Table 1 to improve the calculating cost.

- *Fuzzy inference rules.* In the surveys presented in Section 4 we used 49 laws. Among them there are 18 laws typed NC as in Table 1. For example, the one depicted in Fig. 4 is as below

$$\text{If } S(t) \text{ is } LN \text{ and } \dot{S}(t) \text{ is } SN \text{ then } \bar{k}_{2ad}(t) \text{ is } MN. \tag{18}$$

- *Estimating output value.* There are various methods to achieve this. In this work, the center-point method is adopted to calculate $\bar{k}_{2ad}(t)$ as follows

$$\bar{k}_{2ad}(t) = \frac{\sum_{i=1}^{n} k_{2i}\mu_{B_i'}(k_{2i})}{\sum_{i=1}^{n} \mu_{B_i'}(k_{2i})}, \tag{19}$$

  where N is the number of output fuzzy sets; B_i' is the output fuzzy set corresponding to the i^{th} fuzzy set and dynamic response status of the system at the surveying time; k_{2i} is abscissa of the central point of B_i'.

- *The control force.* By using the result of (19), the control force for the suspension calculated based on $\bar{k}_{2ad}(t)$is given by

$$u(t) = \bar{k}_1 m_m x_2(t) - f_s(x,t) - f_d(x,t) + \bar{k}_{2ad}(t) m_m \,\mathrm{sat}(S(t)) + \hat{d}(t). \tag{20}$$

3.3. Establishing the NUO

As presented in [1], in this system the estimation of $d(x,t)$ can be expressed by $\hat{d}(t)$ via the theory shown in [24] as

$$\hat{d}(t) = z(x,t) + p(x), \tag{21}$$

where $z(x,t)$ is the internal state of the nonlinear observer calculated by

$$\dot{z}(x,t) = -l(x)[g_1 u(t) + g_2 z(x,t) + g_2 p(x) + f(x,t)]. \tag{22}$$

In (21), $p(x)$ is the nonlinear function to be designed; g_1, g_2 and $f(x,t)$ are from (6), while $l(x) = \partial p(x)/\partial x$. By choosing $l(x)$ to be a constant vector, $l(x) = [l_1, ..., l_4]^T \in \Re$, $p(x)$ is then inferred as $p(x) = l(x)^T x(t)$. Whereby $\hat{d}(t)$ is specified as follows

$$\hat{d}(t) = z(x,t) + l(x)^T x(t). \tag{23}$$

From (20) and (23), the control signal for the suspension is calculated as below

$$u(t) = m_m \bar{k}_1 x_2(t) - f_s - f_d + \bar{k}_{2ad}(t) m_m \,\mathrm{sat}(S(t)) + z(x,t) + l(x)^T x(t). \tag{24}$$

4. STABILITY AND CONTROL PERFORMANCE

4.1. Analyzing stability

It can observe that stability of the active suspension system shown in Fig. 1 controlled by the proposed FDIC (24) depends on special features of uncertainty and disturbance (UAD) aspects impacting on the system. When the time varying rate of UAD is slow, the system is asymptotically stable. This can be inferred as follows.

For the FSMC, the FLS_{op} as in Fig. 4 based on the fuzzy rules as in Table 1 makes $\bar{k}_{2ad}(t) > 0$ (see (19)) with the following tendencies. If $S(t) > 0$ then $u(t)$ is increased to reduce $S(t)\Delta S(t)$; if $S(t) \gg 0$, then $u(t)$ is increased quickly to reduce $S(t)\Delta S(t)$ fast. Conversely, if $S(t) < 0$ then $u(t)$ is reduced to reduce $S(t)\Delta S(t)$; if $S(t) \ll 0$ then $u(t)$ is reduced fast to reduce $S(t)\Delta S(t)$ quickly. In case $S(t)\Delta S(t) < 0$ or $S(t) \approx 0$, then there is not any change in $u(t)$ so as to improve the calculating cost. As a result, either $S(t)\Delta S(t) \to 0$ quickly or $S(t)\Delta S(t) < 0$. This is viewed as a necessary condition for the following processes

$$\bar{k}_{2ad}(t)\ \mathrm{sat}(S(t)) \to -\dot{S}(t), \text{ and } \dot{V}(x) < 0. \tag{25}$$

With reference to (7) as well as $V(x) = 0.5\, S(t)^2$, $\dot{V}(x) = S(t)\dot{S}(t)$, taking note of $V(x) \geq 0\ \forall x$ and $V(0) = 0$, in view of Lyapunov stability theory, it can conclude that $S(t) \to 0$ is an asymptotically stable process. Therefore, from (9) and (25) we can infer control law (26) as below

$$u(t) = m_m \bar{k}_1 x_2(t) - f_s - f_d + \bar{k}_{2ad}(t) m_m \,\mathrm{sat}(S(t)) + d(t). \tag{26}$$

Subsequently, related to the NUO we have to prove that

$$\text{if } \dot{d}(t) \to 0 \text{ then } \hat{d}(t) = z(x,t) + p(x) \to d(t). \tag{27}$$

Let $e(t) = d(t) - \hat{d}(t)$ be the estimate error. By using $\hat{d}(t) = z(x,t) + p(x)l(x)$ in which $l(x) = [l_1, ...l_4]^T \in \Re$ is a constant vector, the following equation can be inferred

$$\dot{e}(t) = \dot{d}(t) - \dot{\hat{d}}(t) = \dot{d}(t) - \dot{z}(x,t) - l(x)^T \dot{x}(t). \tag{28}$$

Substituting $\dot{z}(x,t)$ from (22) and $\dot{x}(t)$ from (5) into (28) we have

$$\dot{e}(t) = \dot{d}(t) + l(x)^T g_2\, e(t). \tag{29}$$

From (29) and (6), if UAD is a slow time varying factor, then $\dot{e}(t) + ke(t) = 0$, where $k = l_2/m_m + l_4/m_u$. By choosing $l_{2,4} > 0$ then $k > 0$, so $e(t) = d(t) - \hat{d}(t) \to 0$ or

Table 2. Parameters of the suspension system

m_s = 19600±3000	kg
m_u =1440	kg
k_s =392.10^4	N/m
k_t =2804.10^4	N/m
c_s =5.390.10^4	Ns/m
c_t =6.838.10^4	Ns/m

$\hat{d}(t) = z(x,t) + p(x) \to d(t)$ is an asymptotically stable process. Finally, due to $\hat{d}(t) \to d(t)$, by using the NUO to estimate $d(t)$ in (26) we obtain control law (24). Because both $S(t) \to 0$ and $\hat{d}(t) \to d(t)$ are asymptotically stable processes as presented above, hence the suspension system controlled by the proposed FDIC (24) is asymptotically stable.

Remark 2. For vector $l(x)$, it is noted that the larger value of k will improve better the settling time but the overshoot may reduce the quality of the suspension system. The solution to this is to consider the value of k such that the both terms are appropriately determined. In this work $l(x)$ is chosen as follows $l_1 = 120$, $l_2 = 55$, $l_3 = 18$ and $l_4 = 255$.

4.2. Verifying the method via surveys

In this section, design parameters of the suspension system given in Table 2 are applied to estimate the proposed FDIC. Firstly, three typical track profiles of the railway roads are collected to perform two functions. The first one is to calculate optimal parameters the FDIC. This phase is so-called the training process. The second one is to excite the suspension systems. By this way, the FDIC may only match with the special features of the track profiles used for the training. In order to consider the adaptive ability of the created FDIC, it is then tested via the remainder track profiles. Besides, the passive suspension system as well as another controlable suspension are also employed to compare the obtained surveys with each other. For this work, the controller built based on ANFISs, SMC and uncertainty observer named NFSmUoC presented in [7] is used.

As expressed by Simon [37], real tracks are neither constantly straight nor perfect, and they are collaborated by straights, curves, and track irregularities by different ways. These geometric features of track profiles impact directly on dynamic responses of the railway vehicles. Based on Garg [38], generally a real track profile can be seen as a summation of the isolated track geometry variations consisting of cusp, bump, jog, plateau, trough, sinusoid, and damped sinusoid with track irregularities. The bump-shaped profile with a disturbance surface expresses the locations where two adjacent rails to be connected (joints), or soft spots, washouts, mud spots, fouled ballast, spirals, grade crossings, bridges, overpasses, turnouts and interlockings. The sinusoid profile expresses the track's uneven status at spirals and soft spots. While the track profile like trough with irregularities illustrates special areas such as soft spots, soft and unstable subgrades, or at spirals. In this work, three track profiles, which are combined between the above-mentioned typical track types, are used for experiments. A mathematical model expressing the vertical co-ordinate $x_0(t)x_0(t)$ of a general track profile

containing the abovementioned factors is adopted

$$x_0(t) = \begin{cases} 0.5X_0(1-\cos(\omega t)) & \text{if} \quad 0 \le t \le T/2 \quad \text{or} \quad 3T/2 \le t \le 2T \\ X_0(1+3r) & \text{if} \quad T/2 \le t \le 3T/2 \\ X_0(\sin(0.03\omega t) + \sin(0.2\omega t)) + 3rX_0 & \text{if} \quad t > 2T. \end{cases} \tag{30}$$

In the general track profile (30), $r = |\text{random}(0,\, 0.05)|$ is the positive value chosen randomly distributing around zero with a radius of 0.05, $X_0 = |\text{random}(0,\, 0.01)| \le 0.01$ [m] is the vibration amplitude of the signal which also is chosen randomly such that it distributes around zero with a radius of 0.0. $\omega = k_0(2\pi)/V$ [rad/s] and $T = 2\pi/\omega = V/k_0$ [s], respectively, is the angular frequency and cycle of the surveyed sine-typed road profile in which k_0 is the positive coefficient ($k_0 = 10$ in this work) and V is the proportional rate to be chosen to be equal to the velocity [m/s] of the train in this survey. By choosing three different values of V to be 50, 200 and 250 km/h, three track profiles named track No. 1, 2, 3, respectively are obtained as shown in Fig.5.

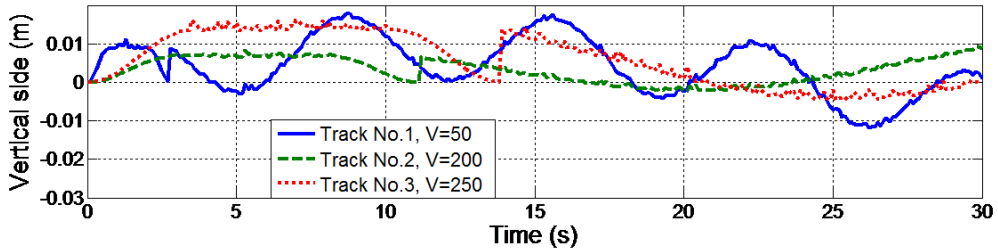

Figure 5. Three track profiles used for surveys

The quantitative analysis is also considered by referring to the standard ISO 2631-1997 which is utilized to test the ride quality by the Association of American Railroads [39]. Guided by the ISO 2631, the magnitude maxima of acceleration, A_a as well as average absolute value of acceleration $\bar{a}$ as depicted in (31) are employed.

$$A_a = \max_{i=1\ldots P} \left|\ddot{z}_s^i\right|; \quad \bar{a} = \frac{1}{p}\sum_{i=1}^{P} \left|\ddot{z}_s^i\right|, \tag{31}$$

where i is the i^{th} data sample; P is the number of data samples.

4.2.1. Survey results

The obtained results coming from the surveys are shown in Figs. 6-9 and Tables 3–4. In Fig. 6, vertical chassis accelerations of the three suspensions excited by Track No.1 in which the FDIC has been trained by one of the three tracks (signed FDIC: TNo.1-ENo.1, or FDIC: TNo.2-ENo.1, or FDIC: TNo.3-ENo.1, respectively) are shown. Be noted that TNo.i-ENo.j reflects the FDIC is trained by Track No. i while the suspension is excited by Track No. j. It is much the same between the contents depicted in Figs. 6-8. The only difference between them is that in Fig. 6 Track No.1 is used to excite the three suspensions, while that in Fig. 7 and Fig. 8 respectively are tracks No.2 and No.3.

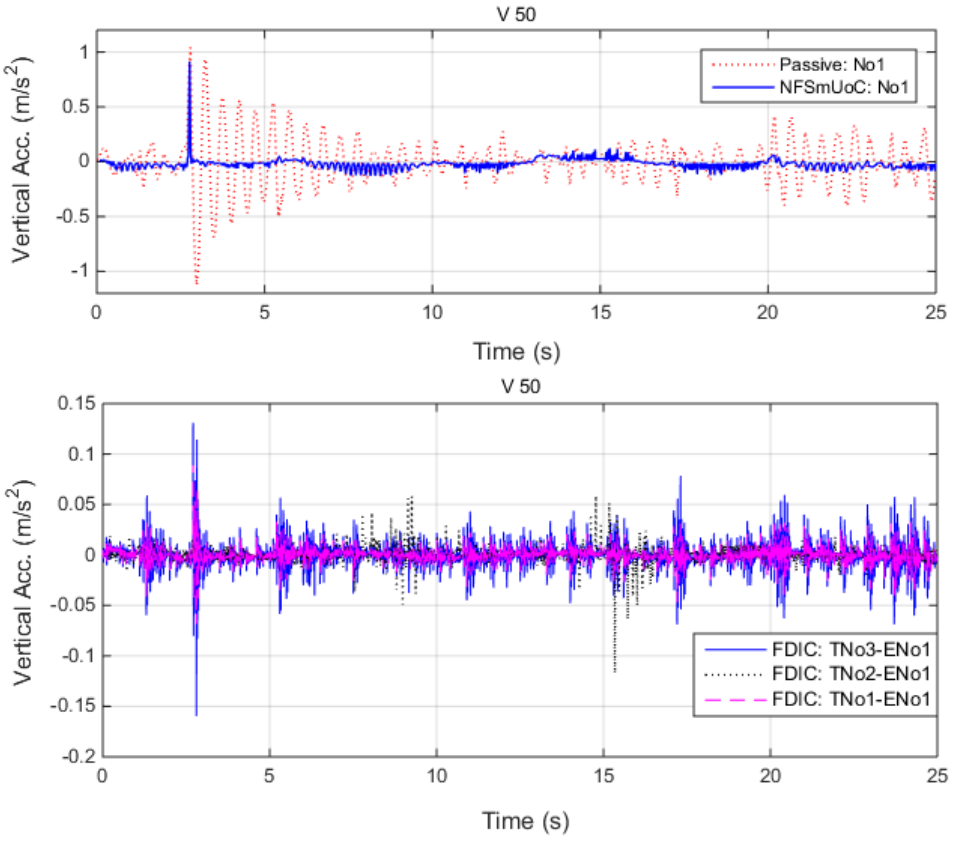

Figure 6. Vertical chassis accelerations of the three suspension systems excited by Track No.1 in which the FDIC has been trained by one of the three tracks (No. 1 or No. 2, or No. 3) signed FDIC: TNo.1-ENo.1, or FDIC: TNo.2-ENo.1, or FDIC: TNo.3-ENo.1, respectively

Besides, the dependence of chassis acceleration on the time-varying rate of the chassis mass ($\dot{d}(t)$) is depicted in Fig. 9. Fig. 9a describes $\dot{d}(t)$ via the angular frequency (f) in case the chassis mass $m_s(t)$ is a function with respect to time, $m_s(t) = 19600 + 1000\sin(ft)$ [kg]. The corresponding chassis accelerations along with some extractions are shown in Fig. 9b and 9c, respectively.

Table 3. Acceleration of the chassis mass excited by one of the three tracks while the FDIC trained via Track No.2

	Track No. 1		Track No. 2		Track No. 3	
	$A_a\,(m/s^2)$	$a\,(m/s^2)$	$A_a\,(m/s^2)$	$a\,(m/s^2)$	$A_a\,(m/s^2)$	$a\,(m/s^2)$
Passive	1.1261	0.1546	0.8477	0.1057	1.6400	0.1786
NFSmUoC	0.9140	0.0356	0.1693	0.0063	0.2291	0.0143
FDIC	**0.1171**	**0.0041**	**0.0960**	**0.0038**	**0.1630**	**0.0071**

Table 4. A_a (m/s^2) of the chassis mass controlled by the FDIC which is trained by Tracks No1-No3 exciting

	Exciting Source		
For training	No. 1	No. 2	No. 3
No. 1	**0.0889**	0.1171	0.1597
No. 2	0.2241	**0.0960**	0.1655
No. 3	0.1028	0.1630	**0.0685**

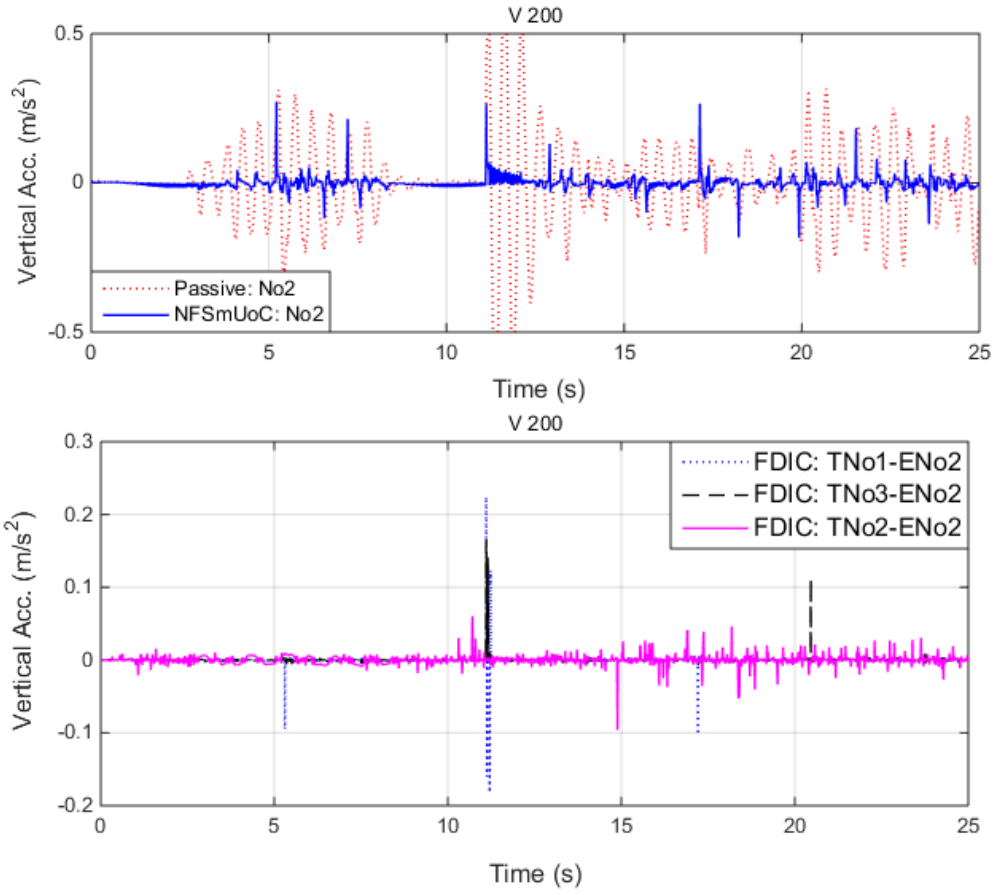

Figure 7. Vertical chassis accelerations of the three suspension systems excited by Track No.2 in which the FDIC has been trained by one of the three tracks (No. 1 or No. 2, or No. 3)

4.2.2. Discussion

The results in Figs. 6-8 and Tables 3–4 reflect accelerations of the chassis mass controlled by the FDIC to be smallest. They are smaller than that deriving from the controller NFSmUoC, and much smaller than that coming from of the passive. The effectiveness is maintained event if FDIC's training tracks are different from the exciting tracks. These

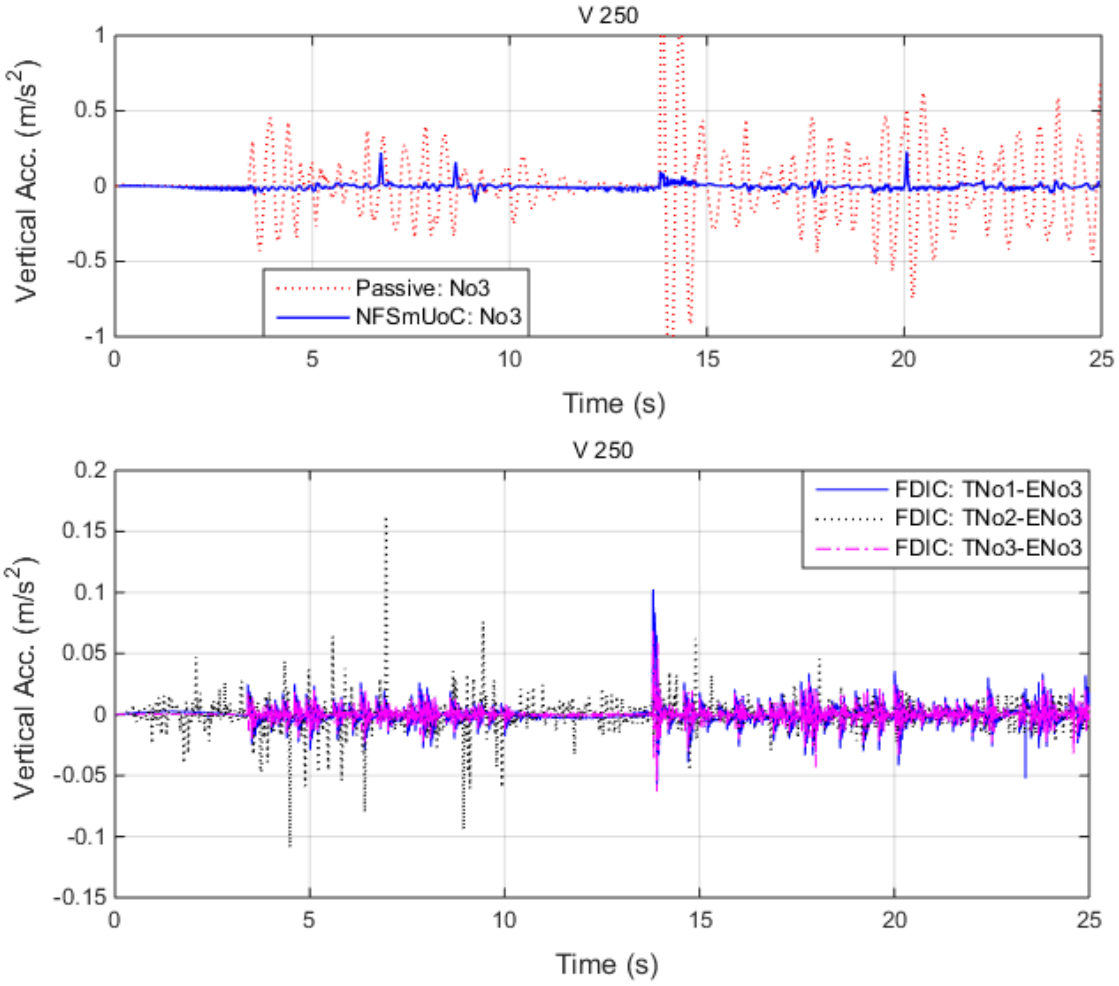

Figure 8. Vertical chassis accelerations of the three suspension systems excited by Track No.3 in which the FDIC has been trained by one of the three tracks (No. 1 or No. 2, or No. 3) signed FDIC: TNo.1-ENo.1, or FDIC: TNo.2-ENo.1, or FDIC: TNo.3-ENo.1, respectively

aspects show that the FDIC is not too sensitive to the features of the training tracks.

Another factor to be the dependence of the chassis acceleration on the time-varying rate of the chassis mass, $\dot{d}(t)$ is described in Fig. 9. Fig. 9 (b), (c) illustrates the increase of both the average absolute acceleration ($\bar{a}$) and maximum absolute acceleration (A_a) when the angular frequency (f) of the chassis mass $m_s(t) = 19600 + 1000\sin(ft)$ increases (or $\dot{d}(t)$ increases). As usual, system dynamic response depends on the time-varying rate of the chassis mass, however, controlled by the proposed FDIC this dependence is not much. It can be seen via Fig. 9 (b) that although A_a grows up fastest when frequency f passes over the value of 3 rad/s to reach to 7 rad/s compared with the other frequency ranges, the changing in A_a is not violent. In case $f = 3$ rad/s, $A_a < 0.1\,\mathrm{m/s^2}$ while $A_a < 0.15\,\mathrm{m/s^2}$ when $f = 7$ rad/s. The disturbance from the chassis mass in these two cases is depicted as in Fig. 10. It should be denoted that for each application, based on the required effectiveness

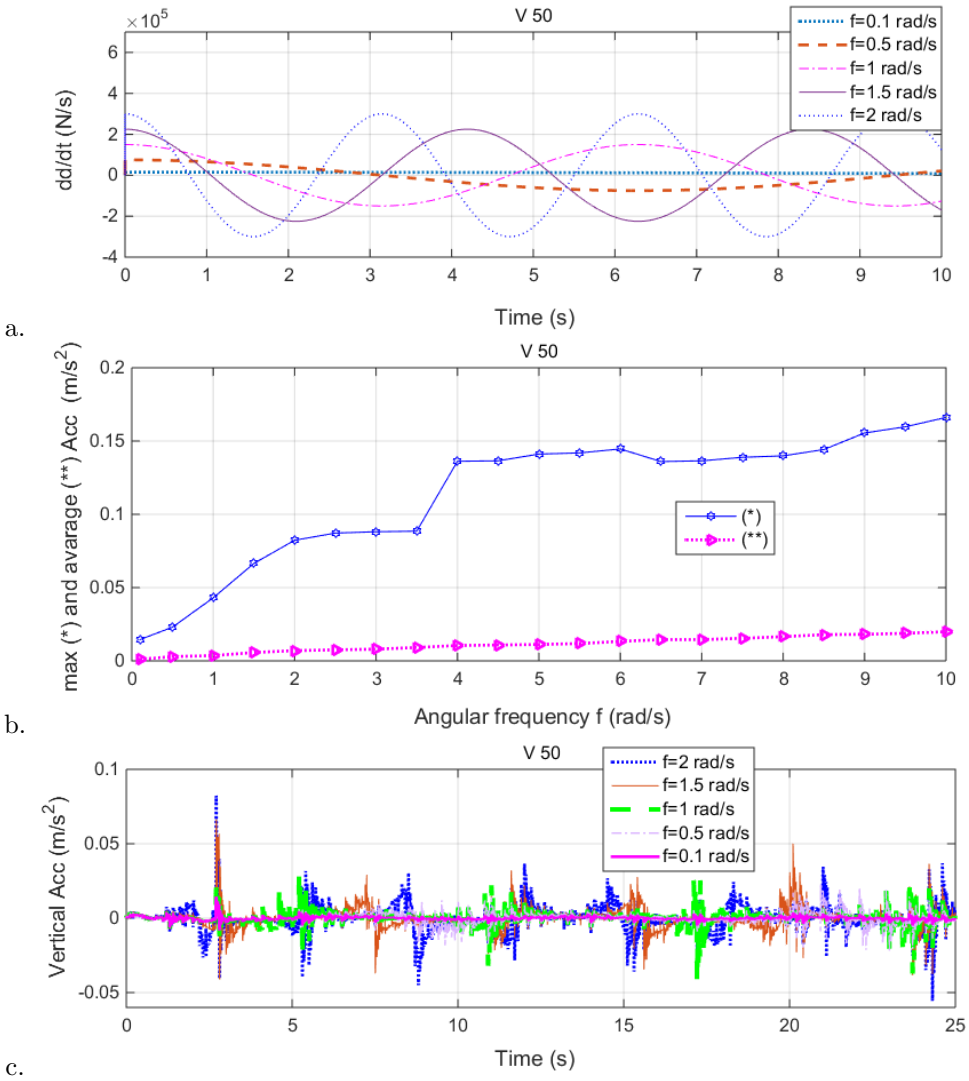

Figure 9. The dependence of chaassis acceleration (and (31)) on the time-varying rate of the chassis mass: (a) is expressed via the angular frequency of the function; (b) the corresponding chassis accelerations; and (c) some extractions

(such as $\bar{a} \leq |\bar{a}|$ or $A_a \leq |A_a|$) of the suspension system and the relation shown in Fig. 9 we can specify specifically the permitted limitation of $\dot{d}(t)$ (or the permitted maximum bound of the time derivative of UAD).

5. CONCLUSION

In this work, in order to deal with the random varying status of the chassis mass, the controller FDIC for the MRD-based train-car suspension systems was formulated. The FDIC consists of three main parts: the ANFIS-I-MRD, FSMC and the NUO. The FSMC is featured by the optimal SMC and the optimal FLS_{op}. The FLS_{op} expanded the ability of the SMC to

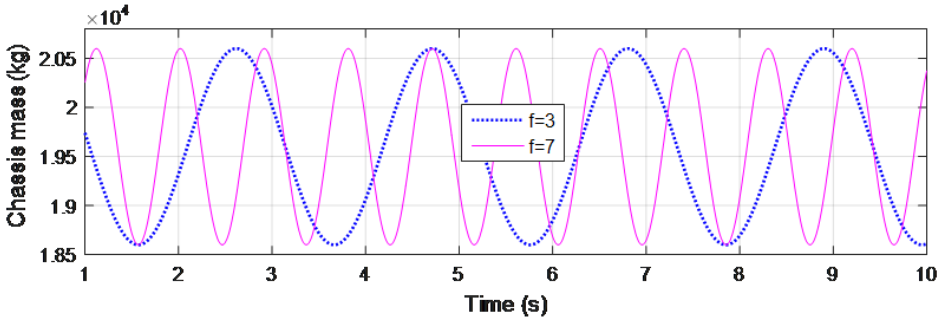

Figure 10. The time-varying chassis mass in the two cases $f = 3$ and $f = 7$

deal with the external disturbance related to the chassis mass and track profile. While the NUO compensated for UAD. By using the ANFIS-I-MRD and the control force estimated by the FDIC, the current for the MRD to stamp out chassis vibration was then determined. The stability of the FDIC was analyzed via Lyapunov stability theory. The effectiveness of the FDIC was validated via a comparative work with the NFSmUoC and the passive method. It has verified that the obtained results from the proposed FDIC can provide considerable ability to extinguish and isolate vibration in the large varying ranges of the chassis mass. The control method is not too sensitive to the features of the track profiles. Based on the method, for each application, the permitted limitation of $\dot{d}(t)$ could be specified if $\bar{a}$ and A_a were given.

ACKNOWLEDGMENT

This research was funded by Vietnam National Foundation for Science and Technology Development (NAFOSTED) under grant number 107.01-2016.22.

REFERENCES

[1] Sy Dzung Nguyen, Hoang Duy Vo and Tae-Il Seo, "Nonlinear adaptive control based on fuzzy sliding mode technique and fuzzy-based compensator," *ISA Transactions*, vol. 70, pp. 309–321, September 2017.

[2] M. A. Karkoub and M. Zribi, "Active/semi-active suspension control using magnetorheological actuators," *International Journal of Systems Science*, vol. 37, pp. 35–44, 2006.

[3] M. Yu, X.M. Dong, S.B. Choi and C.R. Liao, "Human simulated intelligent control of vehicle suspension system with MR dampers," *Journal of Sound and Vibration*, vol. 319, pp. 753–767, 2009.

[4] D.H. Wang and W.H. Liao, "Semi-active suspension systems for railway vehicles using magnetorheological dampers. Part I: system integration and modeling," *Vehicle System Dynamics*, vol. 47, no. 11, pp. 1305–1325, 2009.

[5] X.M. Dong, M. Yu, C.R. Liao and W.M. Chen, "Comparative research on semi-active control strategies for magneto-rheological suspension," *Nonlinear Dyn.*, vol. 59, pp. 433–453, 2010.

[6] S.H. Zareh and A.A.A Khayyat, "Fuzzy inverse model of magnetorheological dampers for semi-active vibration control of an eleven-degrees of freedom suspension system," *J. of System Design and Dyn.*, vol. 5, no. 7, pp. 1485–1497, 2011.

[7] Sy Dzung Nguyen and Quoc Hung Nguyen, "Design of active suspension controller for train cars based on sliding mode control, uncertainty observer and neuro-fuzzy system," *Journal of Vibration and Control*, vol. 23, pp.1334–1353, 2015.

[8] Sy Dzung Nguyen and Seung-Bok Choi, "A new neuro-fuzzy training algorithm for identifying dynamic characteristics of smart dampers," *Smart Materials and Structures*, vol. 21, no. 8, pp. 1–14, 2012.

[9] Sy Dzung Nguyen and Tae-Il Seo, "Establishing ANFIS and the use for predicting sliding control of active railway suspension systems subjected to uncertainties and disturbances," *International Journal of Machine Learning and Cybernetics*, pp.1–13, 2016. DOI 10.1007/s13042-016-0614-z.

[10] J.C. Wu, J.N. Yang, and A.K. Agrawal, "Applications of sliding mode control to benchmark problems," *Earthquake Engineering and Structural Dynamics*, vol. 27, pp. 1247–1265, 1998.

[11] H.C. Cheng, J.L. Cheng, and T.L. Chin, "Nonlinear system control using adaptive neural fuzzy networks based on a modified differential evolution," *Systems, Man, and Cybernetics, Part C: Applications and Reviews, Transactions on IEEE*, vol. 39, no. 4, pp. 459–473, 2009.

[12] V. Nekoukar and A. Erfanian, "Adaptive fuzzy terminal sliding mode control for a class of MIMO uncertain nonlinear systems," *Fuzzy Sets and Systems*, vol. 179, pp. 34–49, 2011.

[13] J.W. Liang, H.Y. Chen, and Q.W. Wu, "Active suppression of pneumatic vibration isolators using adaptive sliding controller with self-tuning fuzzy compensation," *Journal of Vibration and Control*, vol. 21, pp. 246-259, 2015.

[14] M.J Mahmoodabadi, M. Taherkhorsandi, M. Talebipour and V.K.K. Castillo, "Adaptive robust PID control subject to supervisory decoupled sliding mode control based upon genetic algorithm optimization," *Transactions of the Institute of Measurement and Control*, vol. 37, no. 4, pp. 505–514, 2015.

[15] H. Li, J. Yu, C. Hilton, and H. Liu, "Adaptive sliding-mode control for nonlinear active suspension vehicle systems using T–S fuzzy approach," *IEEE Transactions on Industrial Electronics*, vol. 60, no. 8, pp. 3328–3338, 2013.

[16] S.J. Huang and W.C. Lin, "Adaptive fuzzy controller with sliding surface for vehicle suspension control," *IEEE Transactions on Fuzzy Systems*, vol. 11, no. 4, pp. 550–559, 2003.

[17] W. Wang, Y. Song, Y. Xue, H. Jin, J. Hou, and M. Zhao, "An optimal vibration control strategy for a vehicle's active suspension based on improved cultural algorithm," *Applied Soft Computing*, vol. 28, pp. 167–174, 2015.

[18] V.S. Deshpande, B. Mohan, P.D. Shendge, and S.B. Phadke, "Disturbance observer based sliding mode control of active suspension systems," *Journal of Sound and Vibration*, vol. 333, pp. 2281–2296, 2014.

[19] L.C. Felix-Herrana, D. Mehdib, R.A. Ramirez-Mendozaa, Rodriguez-Ortiza and R. Soto, "H2 control of a one-quarter semi-active ground vehicle suspension" *Journal of Applied Research and Technology*, vol. 14, pp. 173–183, 2016.

[20] J. Lin, R. Lian, C. Huang, and W. Sie, "Enhanced fuzzy sliding mode controller for active suspension systems," *Mechatronics*, vol. 19, pp. 1178–1190, 2009.

[21] W. Sun, H. Pan, Y. Zhang, and H. Gao, "Multi-objective control for uncertain nonlinear active suspension system," *Mechatronics*, vol. 24, pp. 318–327, 2014.

[22] H. Pan, X. Jing, and W. Sunb, "Robust finite-time tracking control for nonlinear suspension systems via disturbance compensation," *Mechanical Systems and Signal Processing*, vol. 88, pp. 49–61, 2017.

[23] M.A. Khanesar,O. Kaynak,S. Yin, and H. Gao, "Adaptive indirect fuzzy sliding mode controller for networked control systems subject to time-varying network-induced time delay," *IEEE Trans. on Fuzzy Sys.*, vol. 23, no. 1, 2015.

[24] W.H. Chen, "Nonlinear disturbance observer-enhanced dynamic inversion control of missiles," *Journal of Guidance, Control, and Dynamics*, vol. 26, no. 1, pp. 161–166, 2003.

[25] O. Yakut and H. Alli, "Neural based sliding-mode control with moving sliding surface for the seismic isolation of structures," *Journal of Vibration and Control*, vol. 17, no. 14, pp. 2103–2116, 2011.

[26] V.S. Deshpande, P.D. Shendge, and S.B. Phadke, "Active suspension systems for vehicles based on a sliding-mode controller in combination with inertial delay control," *Proceedings of IMechE, Part D: Journal of Automobile Engineering*, vol. 227, no. 5, pp. 675–690, 2013.

[27] A. Al-khazraji, N. Essounbouli, A. Hamzaoui, F. Nollet, and J. Zaytoon, "Type-2 fuzzy sliding mode control without reaching phase for nonlinear system," *Engin. Applications of Artificial Intelligence*, vol. 24, pp. 23–38, 2011.

[28] P.C. Chen and A.C. Huang, "Adaptive sliding mode control of non-autonomous active suspension systems with time-varying loading," *Journal of Sound and Vibration*, vol. 282, pp. 1119–1135, 2005.

[29] H. Alli and O. Yakut, "Application of robust fuzzy sliding-mode controller with fuzzy moving sliding surfaces for earthquake-excited structures," *Structural Engineering and Mechanics*, vol. 26, no. 5, pp. 517–544, 2007.

[30] Chen and S.J. Huang, "Functional approximation-based adaptive sliding control with fuzzy compensation for an active suspension system," *Proceedings of IMechE, PartD: J. of Automobile Eng.*, vol. 219, pp. 1271–1280, 2005.

[31] R. Storn and K. Price, "Differential evolution – A simple and efficient heuristic for global optimization over continuous spaces," *Journal of Global Optimization*, vol. 11, no. 4, pp. 341–359, 1997.

[32] J. Sun, Q. Zhang, and E.P.K. Tsang, "DE/EDA: A new evolutionary algorithm for global optimization," *Information Sciences*, vol. 169, no. 3/4, pp. 249–262, 2005.

[33] P.P. Menon, J. Kim, D.G. Bates, and Postlethwaite, "Clearance of nonlinear flight control laws using hybrid evolutionary optimization," *Evolutionary Computation, Transactions on IEEE*, vol. 10, no. 6, pp. 689–699, 2006.

[34] W. Gong and Z. Cai, "Differential evolution with ranking-based mutation operators," *IEEE Transactions on Cybernetics*, vol. 43, pp. 1–16, 2013.

[35] Sy Dzung Nguyen, Seung-Bok Choi, and Tae-Il Seo, "Recurrent mechanism and impulse noise filter for establishing ANFIS," *IEEE Transactions on Fuzzy Systems*, vol. 26, pp. 985–997, 2017.

[36] G.C. Hwang and S.C. Lin, "A stability approach to fuzzy control design for nonlinear systems," *Fuzzy Sets Syst.*, vol. 48, pp. 269–278, 1992.

[37] Simon Iwnicki, *Handbook of Railway Vehicle Dynamics*, CRC Press Taylor & Francis Group, 2006.

[38] V.K. Garg, *Dynamics of Railway Vehicle Systems*, Academic Press, Harcourt Brace Jovanovich, Publishers, 1984.

[39] ISO 2631-1997 Mechanical vibration and shock – Evaluation of human exposure to whole-body vibration, Part 1: General requirements, http://www.iso.org/iso/catalogue_detail.htm?csnumber=7612.

Received on October 26, 2017
Revised on March 03, 2018